

https://doi.org/10.1070/QEL17570

System of fibre-optic smoothing of laser radiation on the Luch laser facility

D.V. Sizmin, V.N. Pugacheva, K.V. Starodubtsev, L.A. Dushina,
O.I. Gorchakov, V.N. Derkach, I.N. Voronich

Abstract. **A front end system with spatiotemporal smoothing based on the use of multimode optical fibre has been developed on the Luch laser. The system consists of a broadband master oscillator, a smoothing fibre, preamplifiers, and subsystems for the formation of temporal and spatial radiation profile. The processes of generation of partially coherent radiation, its amplification and conversion into the second harmonic are experimentally investigated. At the amplifying channel output, the pulse energy of the first harmonic reaches up to 1200 J with a pulse duration of 4 ns; the technical coefficient of radiation conversion to the second harmonic is up to 44%, and the beam divergence is 0.2–0.25 mrad. When using smoothed radiation, the speckled structure in the far field is almost completely eliminated: the small-scale inhomogeneity of the target irradiation, integrated over the pulse time, is reduced by 1–2 orders of magnitude compared to unsmoothed radiation.**

Keywords: *smoothing of laser radiation, uniformity of target irradiation, multimode optical fibre, mode dispersion, partially coherent light, speckles.*

1. Introduction

Ensuring the uniformity of the target irradiation is one of the key problems in the physics of the interaction of high-power laser radiation with matter [1], in particular, in experiments on laser-driven inertial confinement fusion (ICF). Small-scale irradiation inhomogeneity (speckles) can lead to parametric instabilities in the target plasma and the generation of hot electrons; it also complicates the interpretation of experimental data.

The general principle of spatiotemporal smoothing of small-scale inhomogeneity of laser radiation is the formation of a speckled intensity distribution that changes rapidly over time. If the time of the distribution change, which is equal in order of magnitude to the coherence time τ_c, is much less than the hydrodynamic response time τ_p of the target plasma, then there occurs an effective averaging of the rapidly alternating speckled pattern. A measure of the target irradiation uniformity can be the contrast of the energy density distribution – the ratio of the root-mean-square deviation (RMS) to its mean value. When averaging $N = \tau_p/\tau_c$ independent random intensity distributions, the contrast decreases by a factor of $\sqrt{N}$.

As a rule, modern Nd : glass lasers of the megajoule energy level use systems of smoothing by spectral dispersion (SSD) [2]. The advantages of this method are the absence (in the ideal case) of amplitude modulation of the beam in the amplifying channel and the possibility of ensuring high efficiency of radiation conversion to the third harmonic. The disadvantages are the need to use microwave phase modulators, the adoption of special measures against the conversion of phase modulation into amplitude modulation in the optical channel, as well as a relatively low degree of smoothing in the one-dimensional version.

An alternative smoothing method is based on decoherenisation of radiation in a multimode optical fibre [3]. The principle of smoothing is as follows. Let a laser pulse with a spectral width $\Delta\nu$ caused by phase fluctuations with a coherence time $\tau_c = 1/\Delta\nu$ be injected into the optical fibre. During the propagation of radiation in the optical fibre, a certain equilibrium distribution of modes is established. The number of modes of one particular radiation polarisation at a wavelength λ in a step-index fibre, core diameter d and numerical aperture NA can be estimated by the formula

$$N_m = \left[\frac{\pi d \mathrm{NA}}{2\lambda}\right]^2. \quad (1)$$

The phase velocities of the modes are approximately evenly distributed in the interval $c/n_2 - c/n_1$, where c is the speed of light in vacuum and $n_{1,2}$ are the refractive indices of the core and cladding. Therefore, the maximum delay time between the 'slowest' and the 'fastest' modes in an optical fibre of length L can be estimated as

$$\Delta t \approx \frac{L}{2cn_1}\mathrm{NA}^2. \quad (2)$$

The modes, combining with random phases at the fibre output, give a speckled intensity distribution with a characteristic speckle size λ/NA. If the average delay time between the modes, equal to $\Delta t/N_m$, is greater than τ_c, the phase differences between the modes at the waveguide output randomly change with the characteristic time τ_c, i.e., a rapidly changing speckled pattern appears. Thus, a multimode fibre of sufficient length converts the temporal incoherence of radiation into a spatiotemporal one.

D.V. Sizmin, V.N. Pugacheva, K.V. Starodubtsev, L.A. Dushina, O.I. Gorchakov, V.N. Derkach, I.N. Voronich Russian Federal Nuclear Center – All-Russian Scientific Research Institute of Experimental Physics (RFNC-VNIIEF), prosp. Mira 37, 607188 Sarov, Nizhny Novgorod region, Russia;
e-mail: oefimova@otd13.vniief.ru; seazmin@yandex.ru

Received 19 April 2021
Kvantovaya Elektronika **51** (8) 687–691 (2021)
Translated by M.A. Monastyrskiy

The advantages of smoothing by optical fibre are the relative simplicity of implementation and a high degree of smoothing in a wide range of spatial frequencies [4], while the disadvantages are 100% modulation of the beam in the amplifying channel at each time moment, as well as low conversion efficiency to the third harmonic, as a result of which this method it is not used in ICF facilities operating in extreme damage threshold regimes. Most experiments on the Luch laser facility [5] are carried out at a moderate energy density (on average, 3–5 J cm^{-2} in the first harmonic at the channel output), which allows working at radiation powers that do not lead to the damage of the optical path elements. In this case, the radiation is converted to the second harmonic, which, when using a KDP crystal, reduces the requirements for the divergence and spectrum width compared to the third harmonic generation; therefore, smoothing by optical fibre can be used on this facility.

2. Front end system with fibre-optic smoothing

The beam forming system (BFS) consists of a broadband master oscillator (MO), optical fibre, preamplifiers, and subsystems for the formation of a temporal and spatial profile (Fig. 1). The electro-optically Q-switched flash-lamp-pumped master oscillator with a neodymium phosphate glass amplifier has a flat resonator with highly reflecting mirrors and a polarisation radiation extraction. The MO parameters are as follows: the pulse energy is 30 mJ, the pulse duration is 17 ns, the radiation wavelength is 1054 nm, and the spectrum width is 2 nm, which corresponds to a coherence time of 1.8 ps. The MO radiation spectrum recorded by a Solar LS SHR high-resolution spectrometer ($\lambda/\Delta\lambda = 30000$) is shown in Fig. 2.

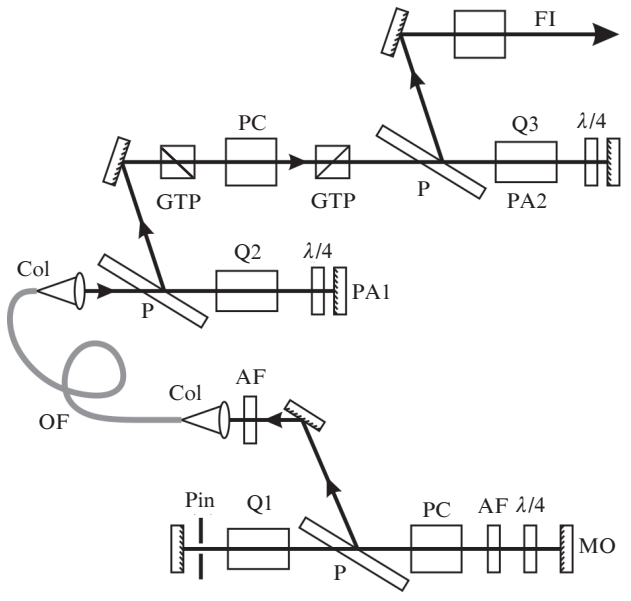

Figure 1. Scheme of the reference radiation formation system with passive spectral smoothing:
(MO) master oscillator; (OF) optical fibre; (PA1, PA2) preamplifiers; (Q1–Q3) quantrons; (PC) Pockels cell; (GTP) Glan–Taylor prism; (λ/4) quarter-wave phase plate; (AF) attenuating filter; (Col) fibre-optic collimator; (P) polariser; (FI) Faraday insulator; (Pin) pinhole.

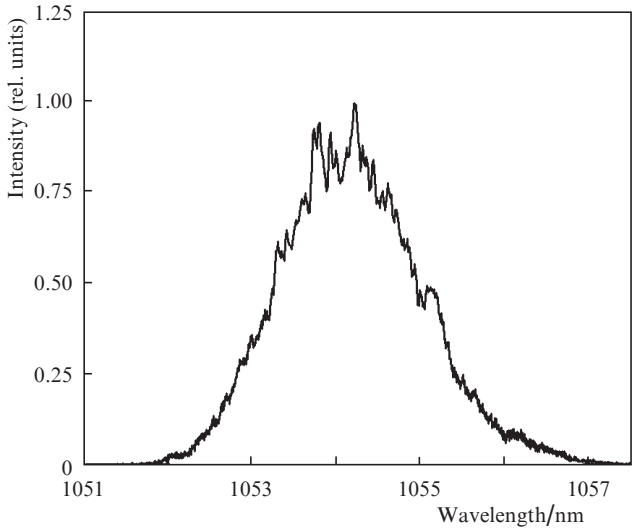

Figure 2. Master oscillator spectrum.

The MO radiation, attenuated to a safe level, is introduced using a fibre-optic collimator into a 100-m-long step-index fibre with a core diameter of 105 μm and a numerical aperture of 0.22. According to formulae (1) and (2), the mode delay is 5.5 ns; if the number of modes exceeds 1000, it should be sufficient for effective smoothing: $\Delta t/N_m \approx 4$ ps $> \tau_c$.

After the laser pulse passes through the fibre, its duration should increase by a time of the order of Δt due to the mode dispersion. However, as shown in Fig. 3a, the output pulse is shorter than the input one by 3–5 ns. With an increase in the input pulse energy, strong power fluctuations appear on the output pulse (Figs 3b and 3c), which may be associated with the effects of nonlinear self-action of radiation in optical fibre. However, the typical pulse power (~100 kW) is an order of magnitude lower than the critical self-focusing power in a silica fibre (~1 MW). It is possible that the MO pulse has a 100% random power modulation with a characteristic time equal to the coherence time. These power fluctuations are not completely resolved by the pulse shape recording system, but their presence can lead to the fact that the instantaneous radiation power reaches a critical value. This effect limits the maximum pulse energy injected into the optical fibre to a level significantly lower than the optical breakdown threshold.

The preamplification system consists of two two-pass amplifiers with a Pockels gate between them, which cuts out a 5 ns pulse, and also provides isolation between the preamplification stages. The preamplifiers' quantrons are the same as in the master oscillator: they have two pump lamps and a ∅6×130 mm neodymium glass rod.

Next, radiation is injected to the main amplifying channel through a serrated aperture [6] and a spatial filter (not shown in Fig. 1), which are part of the standard BFS [7] of the Luch facility and form a square apodised beam. The pulse energy at the path input can be varied by the voltage of the preamplifier pump unit up to 40 mJ.

3. Experimental results

The four-pass amplifying path of each channel of the Luch facility consists of two amplifiers, each containing nine disk active elements made of neodymium phosphate glass. The

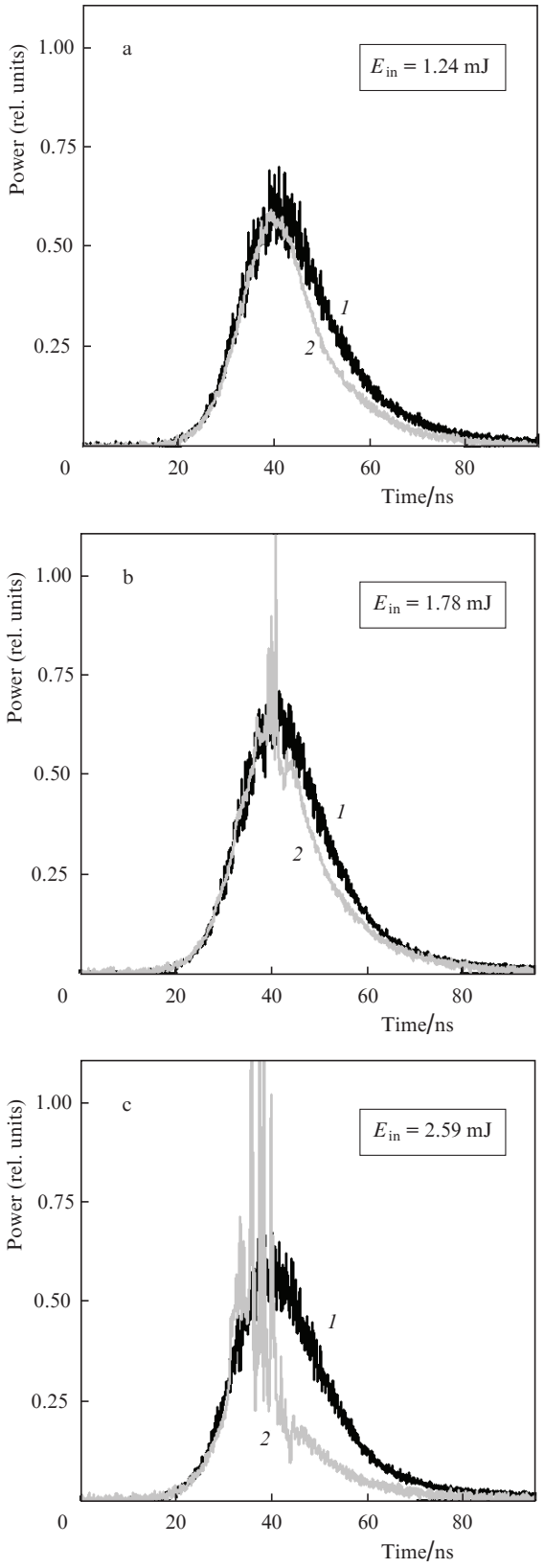

Figure 3. Master oscillator pulse shape (*1*) before and (*2*) after the optical fibre, recorded using photodiodes and an oscilloscope with a 5-GHz bandwidth at different input energies E_{in}.

active elements installed at the Brewster angle have a thickness of 4 cm and are pumped by xenon flash-lamps. Spatial filters are located between the amplifiers.

A series of experiments was performed to amplify the smoothed radiation and convert it into the second harmonic. At the channel output, the pulse energy of the first harmonic ranged from 800 to 1200 J with a beam size of 18 × 18 cm. As can be seen from Fig. 4, the gain of smoothed radiation virtually does not differ from the gain for unsmoothed radiation.

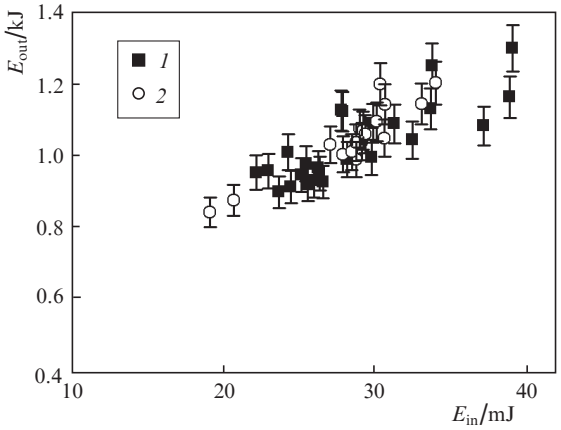

Figure 4. Dependences of the pulse energy E_{out} at the amplifying path output on the input energy E_{in} (*1*) for coherent radiation of the standard BFS and (*2*) for smoothed radiation.

The energy density distribution of the first harmonic beam in the far field (Fig. 5b) is bell-shaped and characterised by the absence of speckles observed in the distribution of unsmoothed radiation (Fig. 5a). The divergence by a level of 80% of the smoothed beam was $(2-2.5)\times10^{-4}$, while the divergence θ_0 of the unsmoothed beam was approximately 1.4×10^{-4}. This difference is due to the multimode nature of the radiation: at the fibre output, the divergence is θ = 1.8NA = 0.4; after increasing the beam cross section by M = 2160 times and adding statistically independent aberrations of the amplifying path, giving the divergence θ_0, the divergence of the smoothed beam turns out to be equal to

$$\theta_s = \sqrt{(\theta/M)^2 + \theta_0^2} = 2.3\times10^{-4}, \quad (3)$$

which is in good agreement with the experimental results.

The experimentally obtained technical coefficient η_{tech} (the ratio of the energy of the second harmonic pulse at the

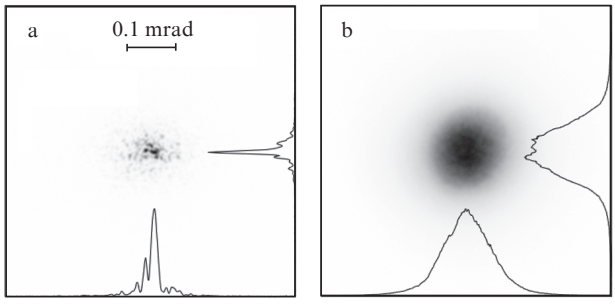

Figure 5. Time-integrated energy density distribution of the first harmonic beam in the far field (a) for the standard BFS radiation and (b) for smoothed radiation.

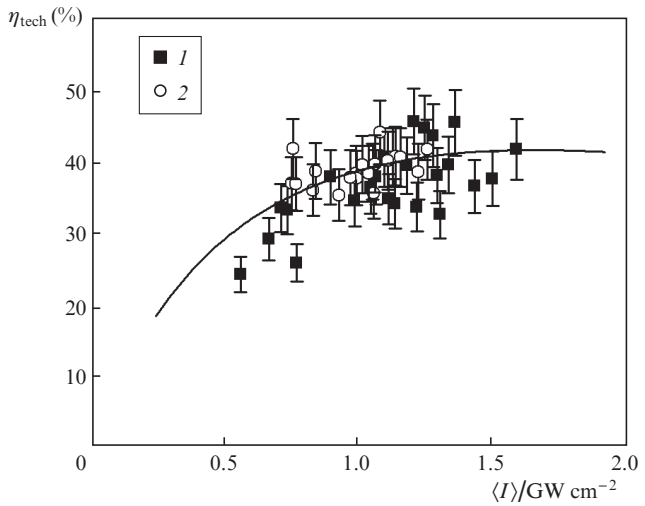

Figure 6. Dependences of the conversion coefficient η_{tech} to the second harmonic on the average beam intensity for (*1*) unsmoothed and (*2*) smoothed radiation at the fundamental harmonic. The solid curve is the simulation for a narrowband unsmoothed beam.

nonlinear crystal output to the energy of the first harmonic pulse incident on the crystal) of the conversion of smoothed radiation into the second harmonic ranged from 36% to 44% at an average radiation intensity of the fundamental frequency of 0.7–1.2 GW cm^{-2} (Fig. 6). Frequency doubling was performed with type-I phase matching in an 18-mm-long KDP crystal with uncoated faces. The conversion coefficient of the smoothed radiation into the second harmonic is approximately the same as that of the unsmoothed radiation, despite the fact that the divergence and the spectrum width of the latter are much smaller.

The radiation converted to the second harmonic passed through a lens raster [8], which, when focused by means of a lens with $F = 1$ m, forms a spot on the target with a size of 600×300 μm. Left panels on Fig. 7 show the time-integrated distributions of radiation on the target, recorded in the equivalent plane. The small-scale inhomogeneity of the spot (speckles) is almost completely eliminated with the use of smoothed radiation. Right panels in Fig. 7 also show the sweeps of the vertical cross-section of the intensity distribution over time, obtained using a streak camera [9]. As can be seen from the streaked images, the speckles do not change their position during the pulse when using narrow-band radiation of the standard BFS, whereas in smoothed radiation, a rapid change in the speckled pattern is observed. The time of characteristic change should be of the order of the coherence time, but we were unable to estimate it experimentally due to insufficient resolution of the streak camera (~70 ps).

If we consider the values of the energy density $Q(x, y)$ of the laser beam at each point on the target surface as a random quantity, the probability density of this quantity can be calculated. The shape of the dependence of the probability density p on the energy density normalised by the average energy density $Q/\langle Q \rangle$ clearly reflects the difference between smoothed and unsmoothed radiation, and the width of the peak $p(Q/\langle Q \rangle$ is proportional to the energy density contrast. Figure 8 allows us to compare the statistical distributions of the experimentally recorded beam

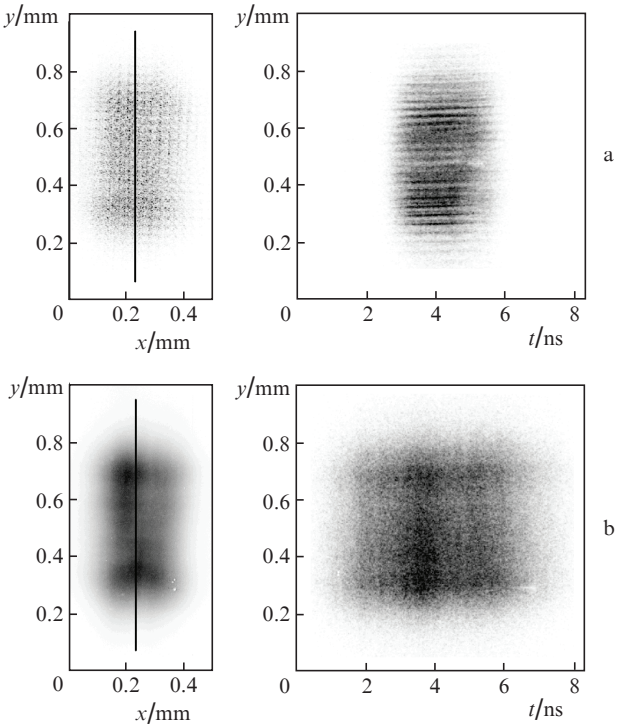

Figure 7. (Left) Energy density distributions on the target and (right) time sweeps of their vertical cross section for (a) unsmoothed and (b) smoothed pulses. The duration of the second harmonic pulse for unsmoothed and smoothed radiation is 2–2.5 ns and about 4 ns, respectively.

energy density on the target, measured in the central part of the spot with a size of 200×400 μm. The contrast of unsmoothed radiation is 58%, while the contrast of smoothed radiation is 17%. The residual contrast of the smoothed spot is associated with large-scale inhomogeneity, which is determined by the beam properties in the near field and the features of the lens raster. The intensity distribution of unsmoothed radiation has statistics close to the Poisson statistics, while that of smoothed radiation is close to the Gaussian one.

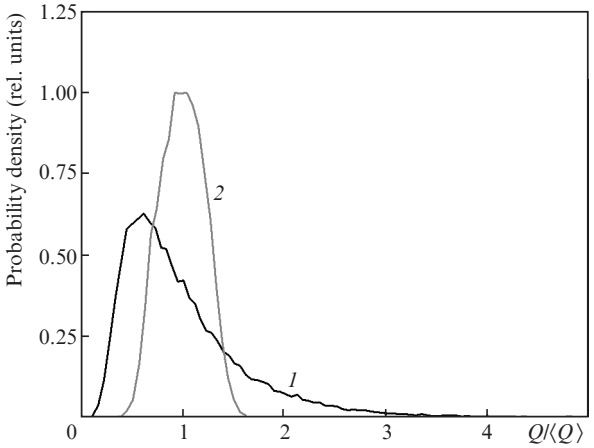

Figure 8. Probability densities of the energy density distribution on the target for (*1*) unsmoothed and (*2*) smoothed radiation.

A comparison of the spatial spectra of the energy density distribution on the target (Fig. 9) shows that the value of small-scale inhomogeneity (with a characteristic size of 100 μm and below) for smoothed radiation is 1–2 orders of magnitude smaller than for unsmoothed radiation.

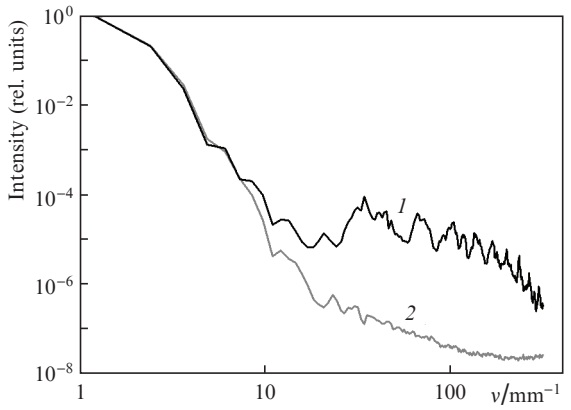

Figure 9. Spatial spectra of the energy density distribution on the target for (*1*) unsmoothed and (*2*) smoothed radiation.

4. Conclusions

Fibre-optic smoothing of laser radiation is a relatively simple and highly efficient method that can be used on kilojoule laser facilities with nanosecond pulse durations, operating with the conversion of radiation into the second harmonic. The level of temporal and spatial coherence of radiation can be controlled using master oscillators with different spectrum widths, as well as by varying the diameter and length of the optical fibre.

Previous attempts to use fibre-optic smoothing on Phebus and Gekko XII facilities did not give the expected results due to a number of problems. For example, in work [10], the saturation of the gain of the smoothed radiation was revealed, which did not allow obtaining the output pulse energy greater than 5.2 kJ (energy density 3.3 J cm^{-2}). The efficiency of frequency doubling in these experiments was up to 27% versus 41% for unsmoothed radiation with an average fundamental harmonic intensity of 1.2 GW cm^{-2}. In experiments [11], the output energy of smoothed radiation reached 700 J (2.2 J cm^{-2}), which is 42% less than for unsmoothed radiation.

We have demonstrated that both the gain at the average energy density at the channel output up to 3.7 J cm^{-2} and the conversion coefficient to the second harmonic, reaching 44% at the average intensity of radiation incident on the crystal of 1.2 GW cm^{-2}, obtained for smoothed radiation, virtually do not differ from those for unsmoothed radiation.

The presented results show the possibility of effective application of smoothing by optical fibre in experiments to study the interaction of laser radiation with matter on the Luch facility. However, it is still necessary to find out the reasons for the anomalous decrease in the duration of the laser pulse when it passes through a multimode optical fibre, to investigate the nonlinear phenomena that occur in this case and limit the transmitted energy, as well as to conduct experimental recording of the rate of change of the speckled pattern on the target with high time resolution.

References

1. Garanin S.G., Derkach V.N., Shnyagin R.A. *Quantum Electron*., **34**, 427 (2004) [*Kvantovaya Elektron*., **34**, 427 (2004)].
2. Skupsky S., Short R.W., Kessler T., et al. *J. Appl. Phys*., **66**, 3456 (1989).
3. Veron D., Ayral H., Gouedard C., et al. *Opt. Commun*., **65**, 42 (1988).
4. Garnier J., Videau L., Gouedard C., Migus A. *J. Opt. Soc. Am. A*, **14**, 1928 (1997).
5. Garanin S.G., Zaretskii A.I., Il'kaev R.I., et al. *Quantum Electron*., **35**, 299 (2005) [*Kvantovaya Elektron*., **35**, 299 (2005)].
6. Belkov S.A., Voronich I.N., Garanin S.G., et al. *Opt. Zh*., **82**, 3 (2015).
7. Rukavishnikov N.N., Savkin A.V., Sharov O.A., et al. *Proc. 27th ECLIM 2002* (Moscow, Russia, 2002) p. 63.
8. Garanin S.G., Kravchenko A.G., Sukharev S.A., et al. *Proc. 29th ECLIM 2007* (Madrid, Spain, 2007) p. 709.
9. Kornienko D.S., Kravchenko A.G., Litvin D.N., et al. *Prib. Tekh. Eksp*., **2**, 79 (2014).
10. Veron D., Thiell D., Gouedard C. *Opt. Commun*., **97**, 259 (1993).
11. Videau L., Boscheron A.C.L., Garnier J., et al. *Proc. SPIE*, **3047**, 757 (1997).